




Research Article

Highly Compact GCPW-Fed Multi-Branch Structure Multi-Band Antenna for Wireless Applications

Ikhlas Ahmad,¹ Wasi Ur Rehman Khan,¹ Sadiq Ullah,¹ Naveed Mufti,¹ Abdullah G. Alharbi ,² Niamat Hussain ,³ Mohammad Alibakhshikenari ,⁴ and Mariana Dalarsson⁵

¹Department of Telecommunication Engineering, University of Engineering and Technology, Mardan, Pakistan

²Department of Electrical Engineering, Faculty of Engineering, Jouf University, Sakaka 42421, Saudi Arabia

³Department of Smart Device Engineering, Sejong University, Seoul 05006, Republic of Korea

⁴Department of Signal Theory and Communications, Universidad Carlos III de Madrid, Leganés 28911, Madrid, Spain

⁵School of Electrical Engineering and Computer Science, KTH Royal Institute of Technology, Stockholm 10044, Sweden

Correspondence should be addressed to Niamat Hussain; niamathussain@sejong.ac.kr and Mohammad Alibakhshikenari; mohammad.alibakhshikenari@uc3m.es

Received 2 April 2022; Revised 22 May 2022; Accepted 31 May 2022; Published 16 June 2022

Academic Editor: Yuan Yao

Copyright © 2022 Ikhlas Ahmad et al. This is an open access article distributed under the Creative Commons Attribution License, which permits unrestricted use, distribution, and reproduction in any medium, provided the original work is properly cited.

In this work, we present a highly compact multi-branch structure multi-band antenna with a grounded coplanar waveguide (GCPW)-fed structure printed on $26 \times 13 \times 1.6 \text{ mm}^3$ sized FR-4 substrate having dielectric constant ϵ_r of 4.3 and loss tangent δ of 0.02. In the proposed antenna, five branches are extended from the main radiator to provide multi-band behavior. Two branches are introduced at the upper end of the main radiator, effectively covering the lower bands, while the other three branches are introduced near the center of the main radiator to extend operation to higher bands. The designed antenna covers five different bands: 2.4 GHz, 4.5 GHz, 5.5 GHz, 6.5 GHz, and 7.8 GHz, with respective gain values of 1.34, 1.60, 1.83, 1.80, and 3.50 dBi and respective radiation efficiency values of 90, 88, 84, 75, and 89%. The antenna shows a good impedance bandwidth, ranging from 170 MHz to 3070 MHz. The proposed antenna is simulated in CST Microwave Studio, while its performance is experimentally validated by the fabrication and testing process. The antenna has potential applications for IoT, sub-6 GHz 5G and WLAN (both enablers for IoT), C-band, and X-band services.

1. Introduction

Due to rapid innovation in communication technologies, new electronic devices are now being designed, with support for multiple wireless applications. This translates into requirements for multiple antennas in a single device, enabling it to perform operations at multiple application-specific bands, leading to a greater size, higher costs, and lower radiation efficiency. An alternative solution is to use multi-band or frequency reconfigurable antennas. Frequency reconfigurable antennas enable communication at various resonant frequencies, using a single antenna structure, thus providing more compact designs [1, 2]. Such antennas involve using active elements (i.e., PIN-diodes, MEMS, and

optical switches) that enable frequency reconfigurability. However, such antennas generally have higher power consumption and costs, with lower radiation efficiency. Another solution is multi-band antennas, which can also perform operations on multiple frequencies, while having compact sizes, low costs, and lower power consumptions [3]. Due to their advantages over simple single-band antennas and frequency reconfigurable antennas, multi-band antennas are considered as suitable candidates for modern communication devices supporting multi-band operations.

In the literature, a lot of work has been carried out on multi-band antennas. In [4], a $55 \times 110 \times 5 \text{ mm}^3$ sized dual band meander line planar inverted-F antenna (PIFA) for cellular applications is presented. The antenna covers

793–962 MHz and 1700–2730 MHz operating bands, with gain and radiation efficiency ranging from 3.34 to 4.19 dBi and 17.03–50.17%, respectively. Similarly, a quad-band PIFA for GSM 1800, GSM 1900, UMTS, Wi-Fi, and cellular applications is presented in [5]. A slotted structured quad-band antenna for mobile phone applications is reported in [6]. It has a compact size of $20 \times 30 \text{ mm}^3$, having a slotted radiator and ground structure and fed by a slotted microstrip line. The antenna covers 1.79–2.63 GHz, 3.46–3.97 GHz, 4.92–5.85 GHz, and 7.87–8.40 GHz ranges, with radiation efficiency ranging from 54 to 86.3%. In [7], a compact $40 \times 20 \text{ mm}^2$ sized dual band monopole antenna is introduced. It operates over 2.42 and 5.34 GHz bands, having respective gain values of 2.05 and 2.83 dBi. A metamaterial-based dual-band antenna supporting LTE, Bluetooth, and WiMAX frequency bands is presented in [8]. It has a branchy structured radiator having two metamaterial unit cells installed on both sides of microstrip feed line. The antenna covers the *L* and *S* bands, while also supporting LTE and WiMAX applications. Similarly, another dual-band metamaterial-based antenna is introduced in [9], resonating at 2.1–3.9 GHz and 5.01–6.4 GHz frequencies. The antenna is a monopole type having a radiator with a thin slot and a metamaterial unit cell loading. In [10], a multi-band, two-element slotted MIMO antenna having composite right/left-handed (CRLH) unit cell loading is introduced. The antenna operates at three different bands (i.e., 2.37–2.64 GHz, 3.39–3.58 GHz, and 4.86–6.98 GHz) and is well suited for multiple WLAN/WiMAX applications. A double layer dual-band antenna covering 2.4 and 3.5 GHz bands is reported in [11]. It has two substrates printed with slotted patches and has a common ground. Due to its large size (i.e., $100 \times 100 \text{ mm}^3$), the antenna can radiate with a good peak gain of 7.4 dBi and has WiMAX and WLAN applications. In [12], a penta-band double slot antenna for WLAN and LTE applications is presented. A dual-band antenna for wireless power transmission is reported in [13], which has a fractal structure and operates at 2.25–2.8 GHz and 5.5–6 GHz bands. In [14], a narrow-band, novel-shaped, resonator-based, quad-band antenna is introduced. It offers high gain unidirectional radiation patterns in 4.6, 5.05, 5.8, and 6.3 GHz bands. Another narrow-band, flower-shaped multi-band, monopole antenna is reported in [15]. The antenna has overall size of $56 \times 59 \times 1.6 \text{ mm}^3$ and resonates at 3.363 GHz, 2.668 GHz, and 1.576 GHz with gain of 3.23, 2.59, and 1.63 dBi, respectively. A meander line-shaped dual-band composite right/left-handed transmission line (CRLH-TL) zeroth-order resonator (ZOR)-based antenna is introduced in [16]. The antenna has $60 \times 90 \text{ mm}^2$ sized ground system, covering 698–960 MHz and 1710–2690 MHz, and is proposed for cellular applications. In [17], a coplanar waveguide (CPW)-fed metamaterial-based tri-band antenna is presented. The antenna uses a split ring resonator (SRR) loaded radiator and a truncated triangular shaped ground. The antenna operates at 5.9 GHz, 3.5 GHz, and 2.4 GHz bands, hence having WLAN and WiMAX applications. However, most of these antennas do not support larger number of frequency bands and services or compromise on size or bandwidth.

In this work, a highly compact grounded CPW-fed branched structure multi-band monopole antenna is presented. The five branches provide multi-band behavior. The proposed antenna exceeds the performance of the antennas discussed in the literature, in terms of number of bands, size, bandwidth, and gain. The prototype has been tested, with the measurement results agreeing well with the simulations.

The rest of the paper is organized as follows. Section 2 describes the methodology of the antenna design. The performance analysis and discussion of the proposed antenna are discussed in Section 3, while the conclusions of the paper are presented in Section 4.

2. Methodology

The proposed radiating structure is a GCPW-fed monopole antenna with five branches introduced to the main radiator to provide the multi-band behavior. Two branches are introduced at upper end of main radiator, to enable operation at lower bands, while other three branches are introduced near the center of main radiator, for higher frequency bands. A finite ground plane is used, for providing good efficiency and better far-field results.

2.1. Antenna Geometry. The geometry of proposed branch structure multi-band antenna is depicted in Figure 1. It is of monopole type, fed by 50Ω GCPW, printed on 1.6 mm thick FR-4 substrate having relative permittivity ϵ_r of 4.3 and loss tangent δ of 0.02. Each of the five branches, introduced to enable the multi-band behavior, tunes to a particular band according to its resonant length. Two branches of lengths ($L_p + L_5 + L_6 + L_7$) and ($S + L_4$) are introduced at upper end of main radiator to allow radiation at intended lower bands. Two other branches of length L_1 and L_2 are introduced on the left side while one branch of length ($A + L_3$) is introduced on the right side of radiator, allowing resonance at intended upper bands. A finite ground is used for better far-field performance. All the dimensions of antenna's geometry are listed in Table 1.

For designing the antenna, the effective resonant lengths for intended resonant frequencies are calculated using transmission line equation [18]. The relationship of resonant length and the respective guided wavelength (λ) is generally given by $L_r = \lambda_g/4$.

2.2. Design Evolution. An overview of the design evolution of the antenna is presented in Figure 2. In Step 1, a simple monopole antenna with a straight pole like radiator of length $L_f = 14.9 \text{ mm}$ is designed. This preliminary design provides a single resonant band of 5.15–7.00 GHz. In the second step, in order to introduce multi-band response and shift the covering band to intended lower frequency band of 2.4 GHz, a 0.70 mm thick branch of length $L_p + L_5 + L_6 + L_7$ is introduced at left top of main radiator. In Step 3, with the objective to shift the upper band to the intended 4.5 GHz frequency, a 0.5 mm thick branch of length $S + L_4$ is introduced at right top of main radiator. In the fourth step, in order to match the antenna for 5.5 GHz band, a tilted

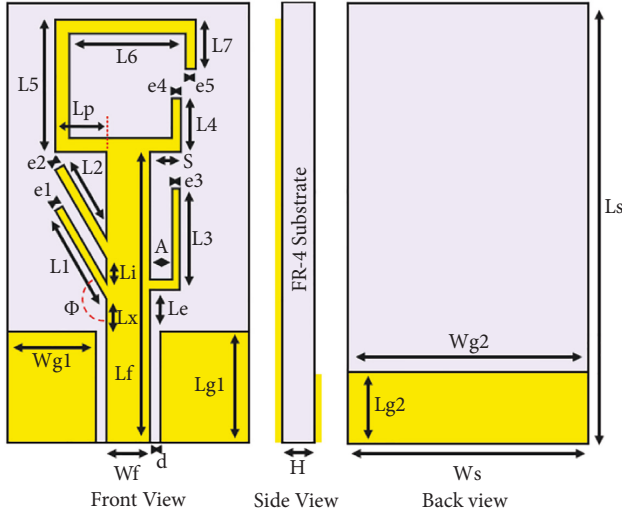


FIGURE 1: Geometry of multi-band antenna.

($\phi = 145^\circ$), 0.5 mm thick branch of length $L2$ is introduced on the left side of main radiator. In Step 5, to add the intended band of 6.5 GHz, another tilted branch of 0.3 mm thickness having length $L1$ is introduced about 0.56 mm below the first tilted one. In the final step, for introducing a wide band of 7.43–10.50 GHz, a 0.5 mm thick branch of length $A + L3$ is introduced in the right-side radiator.

Figure 3 shows all the steps of the design evolution and their respective reflection coefficients. As can be observed, the initial design of the single band antenna has been upgraded to a multi-band antenna through design improvisation.

A summary of supported frequency ranges with respect to steps of antenna design evolution is presented in Table 2.

3. Performance Analysis and Discussion

The antenna is simulated and analyzed using the CST MWS software. The proposed antenna operates at five different bands with good radiation efficiency and gain. The results have been measured at the National University of Sciences and Technology (NUST), using the chamber available at their antenna measurement laboratory. The CST view of the proposed antenna and its prototype during the measurements are shown in Figure 4.

The proposed multi-branch structure antenna has a pentaband response, covering 2.33–2.50 GHz, 4.32–4.72 GHz, 5.34–5.87 GHz, 6.32–7.08 GHz, and 7.43–10.50 GHz bands. In these operating bands, the antenna resonates at 2.4 GHz, 4.5 GHz, 5.5 GHz, 6.5 GHz, and 7.8 GHz, with respective reflection coefficient values of -23 , -26 , -34 , -50 , and -26 dB. The analysis of the measured reflection coefficient shows that the matching impedance of the antenna is good for all intended frequencies. At the respective resonant frequencies, the proposed antenna provides gain of 1.34, 1.60, 1.83, 1.80, and 3.50 dBi and radiation efficiency of 90, 88, 84, 75, and 89%, respectively. The simulated gain ranges from 1.30 to 5.30 dBi while impedance bandwidth ranges from 170 MHz (2.33–2.50 GHz) to 3070 MHz (7.43–10.50 GHz).

TABLE 1: Parameters of the proposed structure.

Parameters	Values (mm)
L_s	26
W_s	13
L_{g1}	6.0
W_{g1}	5.05
L_{g2}	4.0
W_{g2}	13
L_f	14.9
W_f	2.0
$L1$	5.83
$e1$	0.3
$L2$	6.92
$e2$	0.5
$L3$	6.0
$e3$	0.5
$L4$	5.0
$e4$	0.5
$L5$	9.9
$e5$	0.70
$L6$	8.48
$L7$	3.7
L_p	3.95
L_i	0.56
L_x	1.05
L_e	2.0
S	0.9
A	1.0
d	0.45
H	1.6

The comparison between measured and simulated reflection coefficient and gain and radiation efficiency are depicted in Figures 5 and 6, respectively. A good agreement between the measured and simulated results is observed.

The 2D and 3D radiation patterns for all respective resonant frequencies are analyzed. The 2D E and H-plane polar plots are measured in anechoic chamber and compared with simulated results, as shown in Figure 7. The analysis shows that the E-plane radiation pattern resembles a figure of eight, while it seems omnidirectional in pattern and radiates dominantly in the H-plane. The main lobe direction (MLD) and half power beamwidth (HPBW) of E-plane radiation for all resonant frequencies are presented in Table 3.

The simulated co and cross-polar plots at both E and H-planes are illustrated in Figure 8. As depicted in this figure, the antenna offers low values of cross-polarization levels, which makes the proposed antenna a proper candidate for various wireless communication applications with this requirement. For a clearer understanding, 3D radiation plots of all respective frequencies are provided in Figure 9.

The current density over the antenna surface for each resonant frequency is depicted in Figure 10. For the lowest band of 2.4 GHz, it is clearly indicated in respective illustration that most of the area of whole antenna structure is taking part in radiation. In case of 4.5 GHz, main radiator and some parts of upper two branches are contributing to radiation, along with a section of transmission line. In the case of 5.5 GHz, the lower portion of the main radiator and

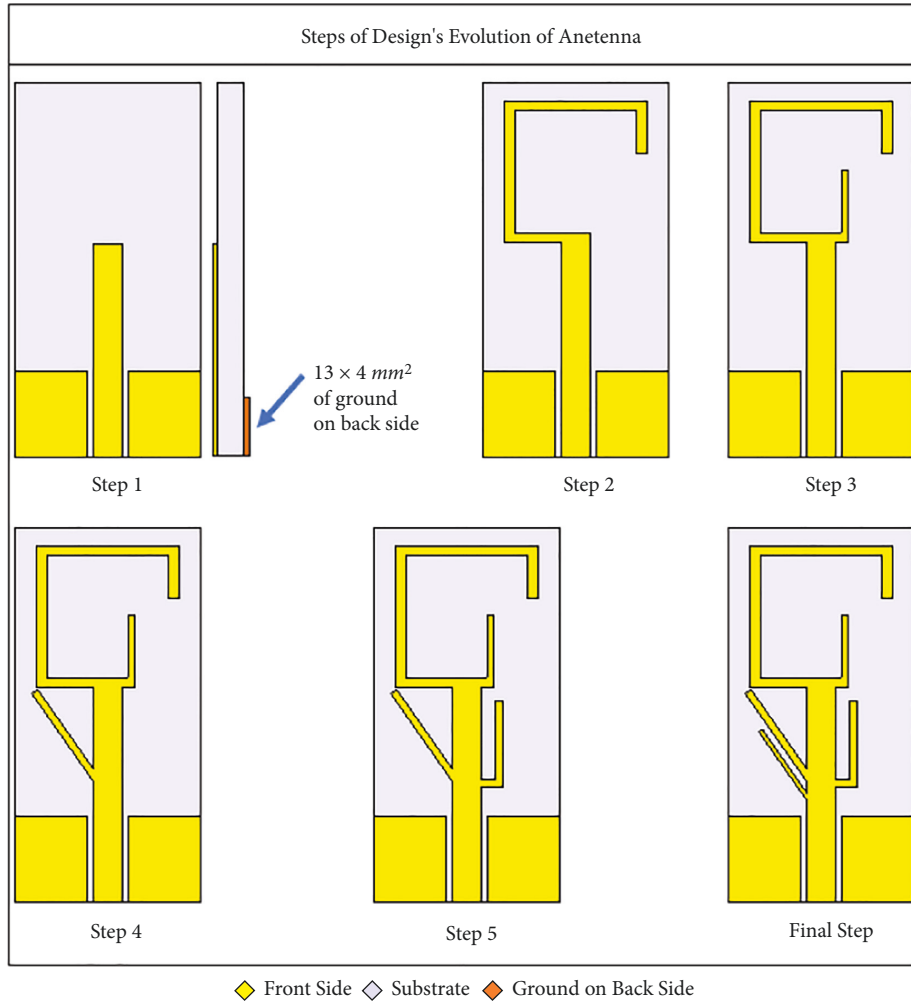


FIGURE 2: Steps of design evolution.

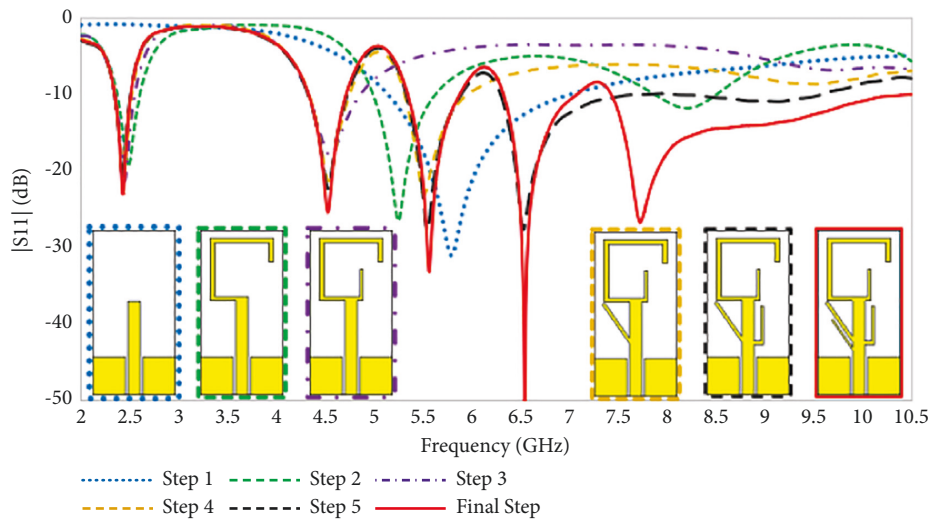


FIGURE 3: Reflection coefficients of various designs of the proposed antenna.

tilted branches are contributing, along with some areas of the transmission line and ground. For 6.5 GHz, it can be observed that the right sided lower branch, while for 7.8 GHz

the tilted smaller branch, is contributing to the radiation along with some areas of the transmission line. While moving from lower toward higher frequencies, the

TABLE 2: Stepwise resonant bands during antenna design.

Steps of evolution	Covering bands (GHz)				
	Band 1	Band 2	Band 3	Band 4	Band 5
1	5.15–7.00	—	—	—	—
2	2.36–2.57	4.98–5.62	—	—	—
3	2.34–2.54	4.31–4.85	—	—	—
4	2.33–2.50	4.32–4.73	5.31–5.95	—	—
5	2.33–2.50	4.32–4.72	5.32–5.88	6.30–7.60	—
Final	2.33–2.50	4.32–4.72	5.34–5.87	6.32–7.08	7.43–10.50

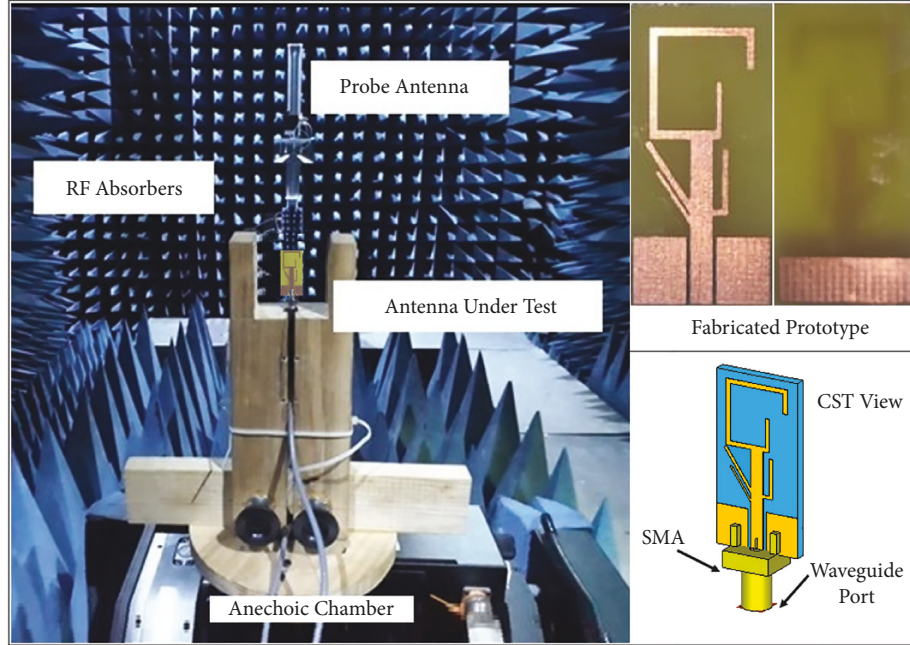


FIGURE 4: Antenna prototype in the measurement phase.

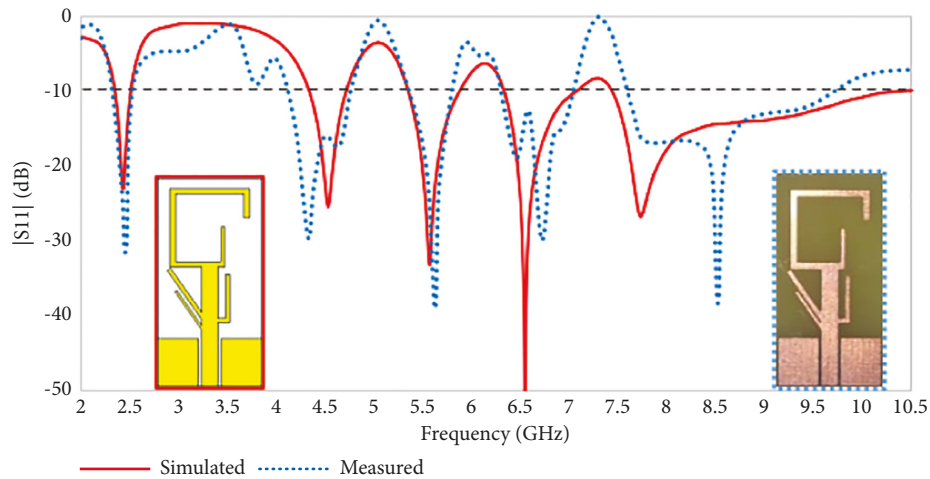


FIGURE 5: Simulated vs. measured reflection coefficient.

respective illustrations clearly indicate a continuous decrease in the contributing resonant area, which proves the inverse relationship of resonant frequency and its contributing resonant area.

The performance of the proposed antenna is summarized in Table 4.

The comparison of the proposed design with relevant previous designs is presented in Table 5. The analytical

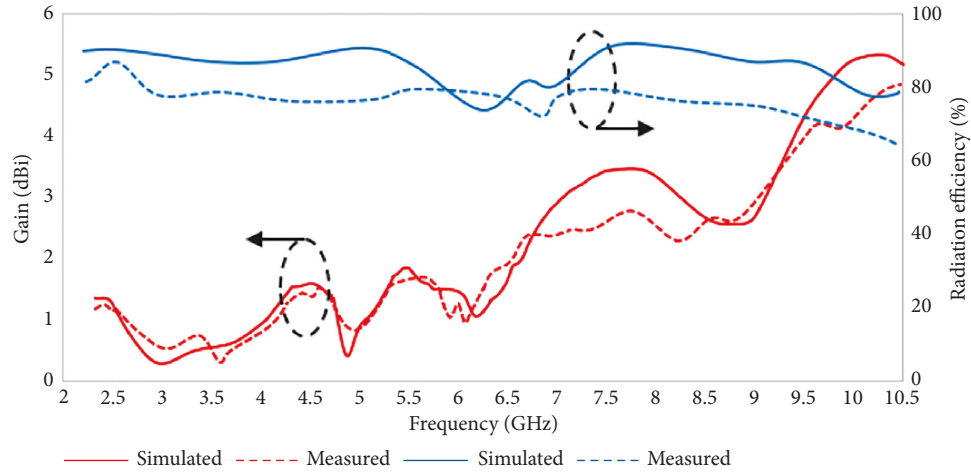


FIGURE 6: Simulated vs. measured gain and radiation efficiency over frequency plot of all operating bands.

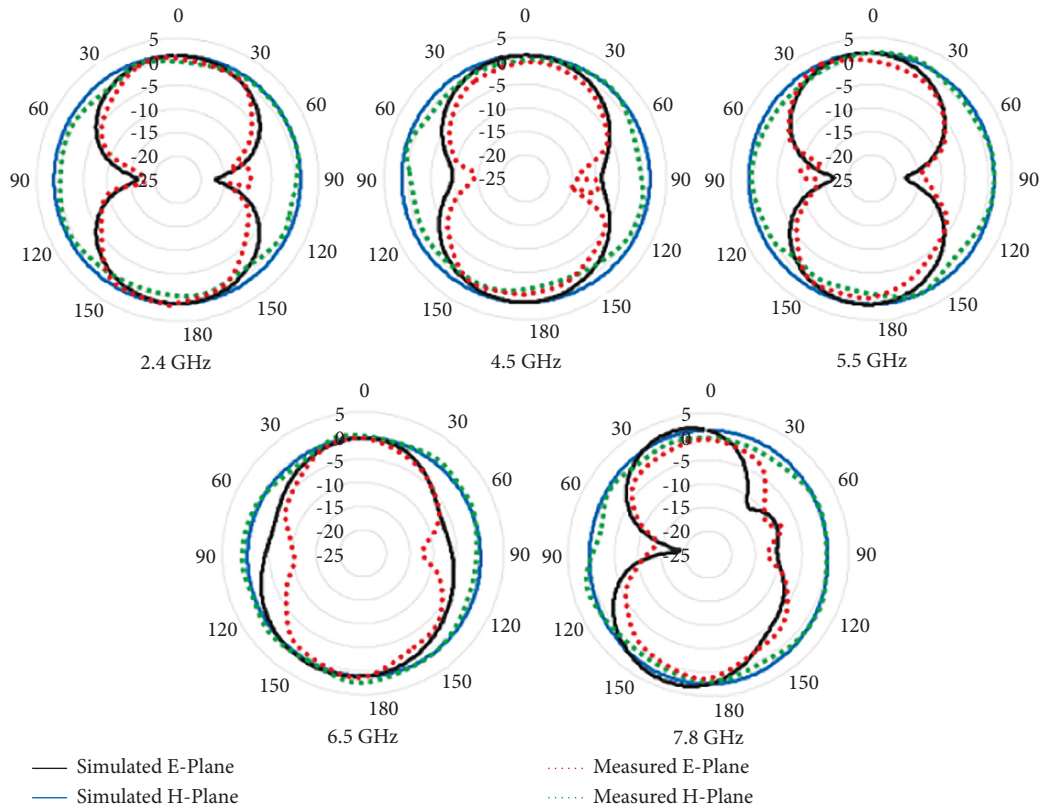


FIGURE 7: Comparison of measured and simulated 2D radiation patterns.

TABLE 3: HPBW and MLD of E-plane radiation pattern of resonant frequencies.

Resonant frequency (GHz)	MLD (in degrees)	HPBW (in degrees)
2.4	180	87
4.5	177	89
5.5	174	74
6.5 7.8	170 163	107 63

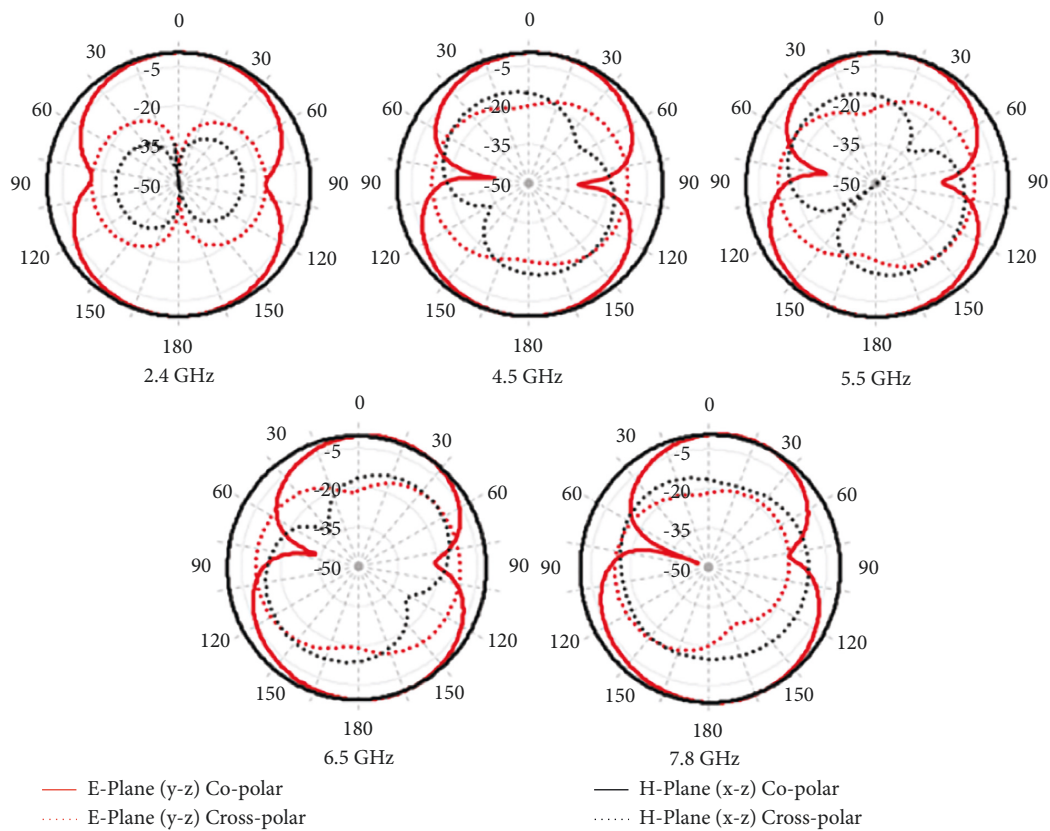


FIGURE 8: Simulated co and cross-polar patterns of the antenna.

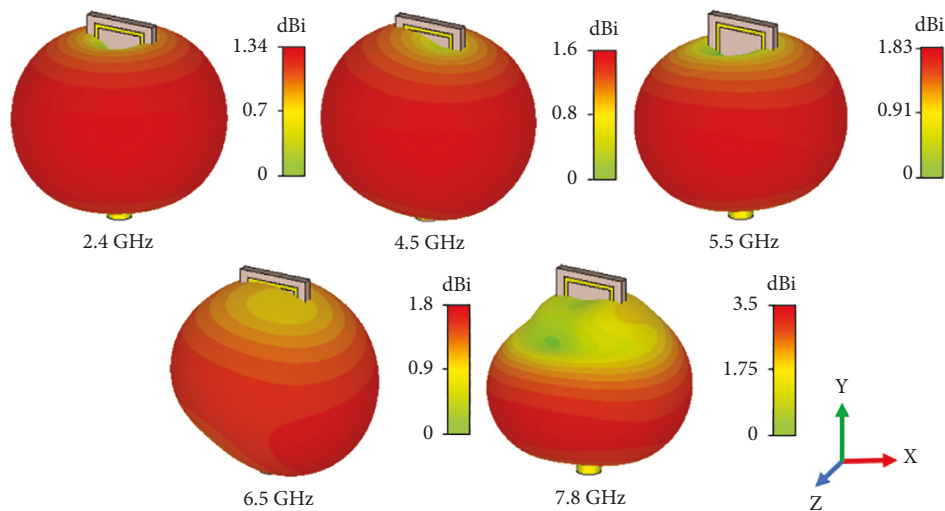


FIGURE 9: Simulated 3D radiation patterns.

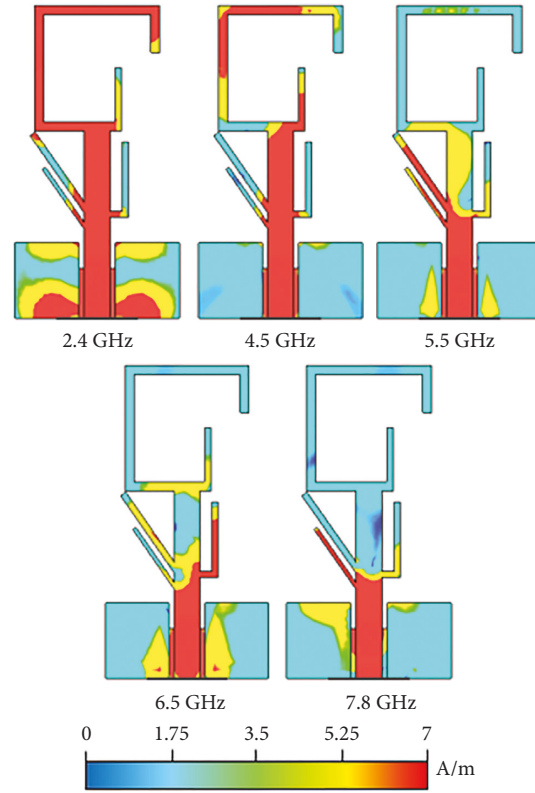


FIGURE 10: Current density distribution for various operating frequencies.

TABLE 4: Summary of various performance parameters.

Resonant frequency (GHz)	Resonant band (GHz)	Gain (dBi)	Radiation efficiency (%)	Reflection coefficient (dB)	VSWR
2.4	2.33–2.50	1.34	90	-23	1.15
4.5	4.32–4.72	1.60	88	-26	1.11
5.5	5.34–5.87	1.83	84	-34	1.05
6.5	6.32–7.08	1.80	75	-50	1.01
7.8	7.43–10.50	3.50	89	-26	1.10

TABLE 5: Performance comparison with relevant previous work.

Ref no.	Size (mm ²)	Electrical dimensions	No. of bands	Resonant bands (GHz)	Bandwidth (MHz)	Gain (dBi)
[6]	40 × 22	0.32 λ × 0.16 λ	2	2.4, 5.4	450, 570	2.05, 2.83
[7]	42 × 32	0.08 λ × 0.06 λ	3	0.6–0.64, 2.67–3.40, 3.61–3.67	40, 730, 60	3.81, 3.75
[8]	45 × 40	0.31 λ × 0.28 λ	2	2.1–3.6, 4.91–6.0	1500, 1090	>2
[10]	100 × 100	0.8 λ × 0.8 λ	2	2.4, 3.5	83, 210	7.1, 7.4
[12]	60 × 30	0.49 λ × 0.24 λ	2	2.45, 5.8	550, 500	2.2, 5.8
[14]	56 × 59	0.29 λ × 0.3 λ	3	1.57, 2.66, 3.63	21, 72.2, 98.9	1.63, 2.59, 3.23
[17]	47 × 45.5	0.147 λ × 0.142 λ	4	0.94, 2.4, 3.5, 5.2	237, 246, 90, 710	2.14, 1.60, 1.45, 4.50
This work	26 × 13	0.208 λ × 0.104 λ	5	2.33–2.50, 4.32–4.72, 5.34–5.87, 6.32–7.08, 7.43–10.50	170, 400, 550, 760, 3070	1.34, 1.60, 1.83, 1.80, 3.50

comparison proves that the presented antenna has better respective performance parameters. In terms of size (mm^2), number of bands, and bandwidth, the proposed antenna outperforms all the designs listed in the table, while good gain values are observed in comparable bands of the antennas presented in [8, 17].

4. Conclusions

A multi-band multi-branch structure antenna is designed, simulated, and experimentally validated by a fabrication and testing process. The proposed antenna is a penta-band antenna, covering the 2.33–2.50 GHz, 4.32–4.72 GHz, 5.34–5.87 GHz, 6.32–7.08 GHz, and 7.43–10.50 GHz bands, with gain values of 1.34, 1.60, 1.83, 1.80, and 3.50 dBi and radiation efficiency values of 90, 88, 84, 75, and 89%, respectively. The antenna shows a wide impedance bandwidth, ranging from 170 MHz to 3070 MHz. Due to its superior performance, the proposed antenna is a strong candidate for future applications in IoT, sub-6 GHz 5G and WLAN (both enablers for IoT), C-band, and X-band applications.

Data Availability

The data used to support the findings of this study are included within the article.

Conflicts of Interest

The authors declare that they have no conflicts of interest.

Acknowledgments

Dr. Mohammad Alibakhshikenari acknowledges support from the CONEX-Plus programme funded by Universidad Carlos III de Madrid and the European Union's Horizon 2020 research and innovation programme under the Marie Skłodowska-Curie grant agreement No. 801538.

References

- [1] S. Ullah, S. Ullah, I. Ahmad et al., "Frequency reconfigurable antenna for portable wireless applications," *Computers, Materials & Continua*, vol. 68, no. 3, pp. 3015–3027, 2021.
- [2] H. Dildar, F. Althobiani, I. Ahmad et al., "Design and experimental analysis of multiband frequency reconfigurable antenna for 5G and sub-6 GHz wireless communication," *Micromachines*, vol. 12, no. 1, p. 32, 2020.
- [3] M. Karthikeyan, R. Sitharthan, T. Ali, and B. Roy, "Compact multiband CPW fed monopole antenna with square ring and T-shaped strips," *Microwave and Optical Technology Letters*, vol. 62, no. 2, pp. 926–932, 2020.
- [4] Y. Hong, J. Tak, J. Baek, B. Myeong, and J. Choi, "Design of a multi-band antenna for LTE/GSM/UMTS band operation," *International Journal of Antennas and Propagation*, vol. 2014, Article ID 548160, 9 pages, 2014.
- [5] R. J. El Bakouchi and A. Ghammaz, "A quad-band compact PIFA operating in the GSM1800/GSM1900/UMTS/LTE2300/LTE2500/2.4-GHz WLAN bands for mobile terminals," in *Proceedings of the 2015 Third World Conference on Complex Systems (WCCS)*, pp. 1–4, IEEE, Marrakech, Morocco, November 2015.
- [6] J. Dong, X. Yu, and G. Hu, "Design of a compact quad-band slot antenna for integrated mobile devices," *International Journal of Antennas and Propagation*, vol. 2016, Article ID 3717681, 9 pages, 2016.
- [7] S. A. A. Shah, M. F. Khan, S. Ullah, A. Basir, U. Ali, and U. Naeem, "Design and measurement of planar monopole antennas for multi-band wireless applications," *IETE Journal of Research*, vol. 63, no. 2, pp. 194–204, 2017.
- [8] M. M. Hasan, M. R. I. Faruque, and M. T. Islam, "Dual band metamaterial antenna for LTE/Bluetooth/Wimax system," *Scientific Reports*, vol. 8, no. 1, p. 1240, 2018.
- [9] S. Chilukuri and S. Gundappagari, "A wide dual-band metamaterial-loaded antenna for wireless applications," *Journal of Electromagnetic Engineering and Science*, vol. 20, no. 1, pp. 23–30, 2020.
- [10] S. Nandi and A. Mohan, "CRLH unit cell loaded triband compact MIMO antenna for WLAN/WiMAX applications," *IEEE Antennas and Wireless Propagation Letters*, vol. 16, p. 1, 2017.
- [11] S. Liu, W. Wu, and D.-G. Fang, "Single-feed dual-layer dual-band E-shaped and U-slot patch antenna for wireless communication application," *IEEE Antennas and Wireless Propagation Letters*, vol. 15, pp. 468–471, 2016.
- [12] M.-C. Chang and W.-C. Weng, "A printed multi-band slot antenna for LTE/WLAN applications," in *Proceedings of the 2015 IEEE International Symposium on Antennas and Propagation & USNC/URSI National Radio Science Meeting*, pp. 1144–1145, IEEE, Vancouver, BC, Canada, July 2015.
- [13] T. Benyetho, J. Zbitou, L. El Abdellaoui, H. Bennis, and A. Tribak, "A new fractal multiband antenna for wireless power transmission applications," *Active and Passive Electronic Components*, vol. 2018, Article ID 2084747, 10 pages, 2018.
- [14] C.-X. Mao, S. Gao, Y. Wang, and B. Sanz-Izquierdo, "A novel multiband directional antenna for wireless communications," *IEEE Antennas and Wireless Propagation Letters*, vol. 16, pp. 1217–1220, 2017.
- [15] S. Ullah, F. Faisal, A. Ahmad, U. Ali, F. A. Tahir, and J. A. Flint, "Design and analysis of a novel tri-band flower-shaped planar antenna for GPS and WiMAX applications," *Journal of Electromagnetic Waves and Applications*, vol. 31, no. 9, pp. 927–940, 2017.
- [16] C. Huang, Y.-C. Jiao, Z.-B. Weng, and X. Li, "A planar multiband antenna based on CRLH-TL ZOR for 4G compact mobile terminal applications," in *Proceedings of the 2018 International Workshop on Antenna Technology (iWAT)*, pp. 1–3, IEEE, Nanjing, China, March 2018.
- [17] O. M. Dardeer, H. Elsadek, and E. A. Abdallah, "CPW-fed multiband antenna for various wireless communications applications," in *Proceedings of the 2018 IEEE International Symposium on Antennas and Propagation*, pp. 785–786, IEEE, Boston, MA, USA, July 2018.
- [18] C. A. Balanis, *Antenna Theory: Analysis and Design*, John Wiley & Sons, Hoboken, 2015.